

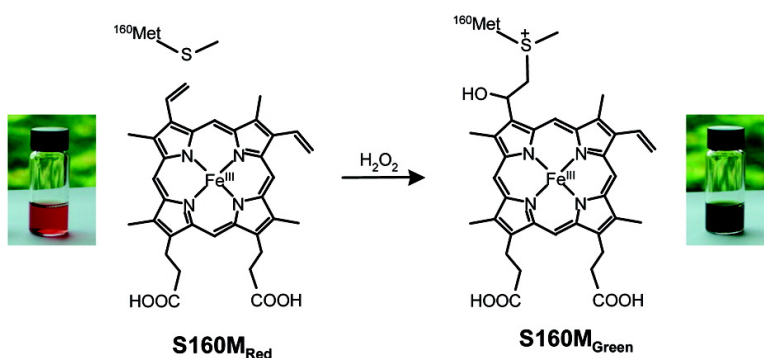
Article

## Autocatalytic Formation of Green Heme: Evidence for HO-Dependent Formation of a Covalent Methionine–Heme Linkage in Ascorbate Peroxidase

Clive L. Metcalfe, Michael Ott, Neesha Patel, Kuldip Singh, Sharad C. Mistry, Harold M. Goff, and Emma Lloyd Raven

*J. Am. Chem. Soc.*, **2004**, 126 (49), 16242-16248 • DOI: 10.1021/ja048242c • Publication Date (Web): 16 November 2004

Downloaded from <http://pubs.acs.org> on April 5, 2009



### More About This Article

Additional resources and features associated with this article are available within the HTML version:

- Supporting Information
- Links to the 4 articles that cite this article, as of the time of this article download
- Access to high resolution figures
- Links to articles and content related to this article
- Copyright permission to reproduce figures and/or text from this article

[View the Full Text HTML](#)

## Autocatalytic Formation of Green Heme: Evidence for H<sub>2</sub>O<sub>2</sub>-Dependent Formation of a Covalent Methionine–Heme Linkage in Ascorbate Peroxidase

Clive L. Metcalfe,<sup>†</sup> Michael Ott,<sup>§</sup> Neesha Patel,<sup>†</sup> Kuldip Singh,<sup>†</sup> Sharad C. Mistry,<sup>‡</sup> Harold M. Goff,<sup>§</sup> and Emma Lloyd Raven<sup>\*†</sup>

Contribution from the Department of Chemistry, University of Leicester, University Road, Leicester LE1 7RH, U.K., Protein and Nucleic Acid Chemistry Laboratory, Hodgkin Building, University of Leicester, Lancaster Road, Leicester LE1 9HN, U.K., and Department of Chemistry, 305 Chemistry Building, The University of Iowa, Iowa City, Iowa 52242-1294

Received March 27, 2004; E-mail: emma.raven@le.ac.uk

**Abstract:** The mammalian heme peroxidases are distinguished from their plant and fungal counterparts by the fact that the heme group is covalently bound to the protein through ester links from glutamate and aspartate residues to the heme 1- and 5-methyl groups and, in the case of myeloperoxidase, through an additional sulfonium link from the C<sub>β</sub> of the 2-vinyl group to a methionine residue. To duplicate the sulfonium link in myeloperoxidase and to obtain information on its mechanism of formation, we have engineered a methionine residue close to the 2-vinyl group in recombinant pea cytosolic ascorbate peroxidase (rpAPX) by replacement of Ser160 by Met (S160M variant). The S160M variant is isolated from *Escherichia coli* as apo-protein. Reconstitution of apo-S160M with exogenous heme gives a red protein (S160M<sub>R</sub>) which has UV-visible ( $\lambda_{\text{max}}/\text{nm} = 407, 511, 633$ ) and steady-state kinetic ( $k_{\text{cat}} = 156 \pm 7 \text{ s}^{-1}$ ,  $K_{\text{M}} = 102 \pm 15 \mu\text{M}$ ) properties that are analogous to those of rpAPX. The reaction of S160M<sub>R</sub> with H<sub>2</sub>O<sub>2</sub> gives a green protein (S160M<sub>G</sub>). Electronic spectroscopy, mass spectrometry, and HPLC analyses are consistent with the formation of a covalent linkage between the methionine residue and the heme vinyl group in S160M<sub>G</sub>. Single-wavelength and photodiode array stopped-flow kinetic analyses identify a transient Compound I species as a reaction intermediate. The results provide the first direct evidence that covalent heme linkage formation occurs as an H<sub>2</sub>O<sub>2</sub>-dependent process that involves Compound I formation. A mechanism that is consistent with the data is presented.

### Introduction

The mammalian heme peroxidases, the most well-known examples of which are myeloperoxidase (MPO) and lactoperoxidase (LPO), are distinguished from their plant and fungal counterparts by virtue of a covalently bound heme group. There is a long history associated with attempting to elucidate the structural details of these covalent links,<sup>1–4</sup> but the chemical identity of the covalent linkages was eventually revealed by spectroscopic work on LPO,<sup>5,6</sup> which showed two ester links from glutamate and aspartate residues to the heme 1- and 5-methyl groups. Structural<sup>7</sup> and spectroscopic<sup>8,9</sup> work later

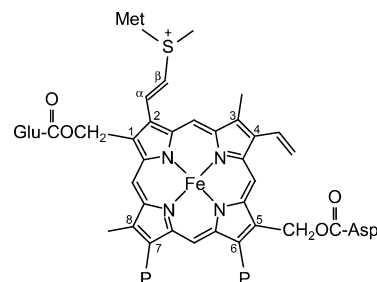


**Figure 1.** Structure of the heme group in MPO (P = propionate). LPO contains the same heme structure, but lacks the vinyl–methionine link.

revealed that MPO contains the same ester linkages but has an additional sulfonium link from the C<sub>β</sub> of the 2-vinyl group to a methionine residue, Figure 1. There is now convincing evidence that the unusual ester linkages are used more widely in other mammalian heme peroxidases,<sup>10,11</sup> and the same covalent attachment has also been identified in the CYP4 family of cytochrome P450 enzymes.<sup>12,13</sup>

<sup>†</sup> Department of Chemistry, University of Leicester.

<sup>‡</sup> Protein and Nucleic Acid Chemistry Laboratory, University of Leicester.

<sup>§</sup> The University of Iowa.

- (1) Morell, D. B. *Aust. J. Exp. Biol. Med. Sci.* **1953**, *31*, 567.
- (2) Morell, D. B. *Biochim. Biophys. Acta* **1963**, *71*, 157–164.
- (3) Nichol, A. W.; Angel, L. A.; Moon, T.; Clezy, P. S. *Biochem. J.* **1987**, *247*, 147–150.
- (4) Hultquist, D. E.; Morrison, M. *J. Biol. Chem.* **1963**, *238*, 2843–2846.
- (5) Rae, T. D.; Goff, H. M. *J. Am. Chem. Soc.* **1996**, *118*, 2103–2104.
- (6) Rae, T. D.; Goff, H. M. *J. Biol. Chem.* **1998**, *273*, 27968–27977.
- (7) Fiedler, T. J.; Davey, C. A.; Fenna, R. E. *J. Biol. Chem.* **2000**, *275*, 11964–11971.
- (8) Kooter, I. M.; Pierik, A. J.; Merckx, M.; Averill, B. A.; Moguilevsky, N.; Bollen, A.; Wever, R. *J. Am. Chem. Soc.* **1997**, *119*, 11542–11543.
- (9) Kooter, I. M.; Moguilevsky, N.; Bollen, A.; van der Veen, L. A.; Otto, C.; Dekker, H. L.; Wever, R. *J. Biol. Chem.* **1999**, *274*, 26794–26802.

(10) Oxvig, C.; Thomsen, A. R.; Overgaard, M. T.; Sorensen, E. S.; Hojrup, P.; Bjerrum, M. J.; Gleich, G. J.; Stottrop-Jensen, L. *J. Biol. Chem.* **1999**, *274*, 16953–16958.

(11) Fayadat, L.; Niccoli-Sire, P.; Lanet, J.; Franc, J.-L. *J. Biol. Chem.* **1999**, *274*, 10533–10538.

There is no detailed information on the mechanism of covalent linkage formation in the mammalian peroxidases. This is an important question not only because it underpins our more general understanding of the chemical, biological, and biomedical properties of the mammalian enzymes, but also because it is relevant to our understanding of covalent heme formation in other proteins. The ester links in LPO are likely generated autocatalytically, by reaction with  $\text{H}_2\text{O}_2$ ,<sup>14,15</sup> but no reaction intermediates have been detected. The ester links have recently been engineered into horseradish peroxidase.<sup>16</sup> There is no information at all on the mechanism of formation of the sulfonium ion linkage. To address this deficiency and to duplicate the sulfonium link seen in MPO, we have engineered a methionine residue close to the 2-vinyl group in recombinant pea cytosolic ascorbate peroxidase (rpAPX). The results provide the first direct evidence that covalent linkage formation between the methionine residue and the heme vinyl group occurs as an  $\text{H}_2\text{O}_2$ -dependent process, and they identify a transient Compound I species as a reaction intermediate for the first time.

## Experimental Procedures

**Materials.** Hydrogen peroxide solution (33%) was purchased from BDM laboratory supplies. All molecular biology kits and enzymes were used according to manufacturer protocols. Oligonucleotide synthesis and DNA sequencing was carried out by the Protein and Nucleic Acid Laboratory at the University of Leicester. Water was purified from an Elga purelab purification system, and all buffers were filtered through a 0.2  $\mu\text{m}$  filter before use.

**Molecular Modeling.** The X-ray crystal structure of recombinant cytosolic pea APX (rpAPX) was analyzed using a Swiss-pdb viewer v.3.7 (1995–2001 N. Guex), and all residues within 5 Å of the  $\beta$ -carbon of the 2-vinyl group of the heme active site were identified. These candidates were mutated within the program to a methionine, and the side chain was energy minimized within a Swiss-pdb viewer.

**Mutagenesis, Protein Expression, and Purification.** The rpAPX gene from the pMal2c vector<sup>17</sup> was modified by PCR to introduce 5'-*Bam*HI and 3'-*Hind*III sites and was subcloned into the pQE30 plasmid, such that the expressed N-terminal sequence was MRGSHHHHH-HGSGK- (with the last residue corresponding to lysine-3 of the wild-type protein). DNA sequencing of the entire coding region confirmed that no mutations had occurred, but a silent mutation was observed at Pro178 (CCA to CCG). The expression construct was transformed into *E. coli* SG13009 p[REP4] cells (Qiagen). Site-directed mutagenesis was performed using a Quikchange mutagenesis kit (Stratagene) according to the manufacturer's instructions. For the S160M mutation, the primers were: 5'-ATTGTTGCTCTAATGGGTGGTCACACC-3' (forward primer) and 5'-GGTGTGACCACCCATTAGAGCAACAAT-3' (reverse primer), with the mutation shown in bold. To confirm the identity of the transformants, overnight cultures containing 100  $\mu\text{g mL}^{-1}$  ampicillin (Sigma-Aldrich) and 25  $\mu\text{g mL}^{-1}$  kanamycin (Sigma-Aldrich) were incubated at 37 °C with vigorous shaking. The plasmid DNA was isolated using the Qiagen mini-prep plasmid system. The mutation was confirmed by sequencing across the entire rpAPX coding gene.

The overexpression of S160M was achieved as follows: Two 200 mL aliquots of LB media containing 100  $\mu\text{g mL}^{-1}$  ampicillin and 25

$\mu\text{g mL}^{-1}$  kanamycin were inoculated with single SG13009 *E. coli* colonies transformed with the S160M gene. These cultures were grown overnight to the late log phase at 37 °C, and 50 mL samples were used to inoculate a further eight 1 L cultures containing 100  $\mu\text{g mL}^{-1}$  ampicillin and 25  $\mu\text{g mL}^{-1}$  kanamycin. These cultures were grown at 37 °C until their OD<sub>600</sub> reached 0.9, and then protein expression was induced by adding isopropyl- $\beta$ -D-thiogalactopyranoside (Sigma) to a final concentration of 1 mM with the temperature lowered to 30 °C. After 14 h of fermentation, the cells were harvested by centrifugation, resuspended in sonication buffer (50 mM potassium phosphate, pH 8.0, 300 mM potassium chloride, 10% glycerol), and lysed by ultrasonication. Purification of the S160M variant was achieved using Ni-NTA agarose resin (Qiagen) according to the manufacturer's instructions, but elution of the protein was using low pH buffer (pH 4.2) and not imidazole and was isolated as apo-enzyme. Reconstitution with heme was as described previously.<sup>18</sup> Excess heme was removed using Fast Flow Q-Sepharose anion-exchange resin (Amersham Pharmacia Biotech) (elution with 250 mM potassium chloride). A high molecular weight impurity was removed with FPLC using a Superdex HR75 size exclusion column (isocratic gradient of 150 mM potassium phosphate buffer, pH 7.0, flow rate of 0.2 mL/min). The purified enzyme showed an  $A_{\text{oret}}/A_{280}$  ratio > 2.0 and migrated as a single band on SDS-PAGE.

**Electronic Absorption Spectroscopy.** Spectra were collected using a Perkin-Elmer Lambda 35 or 40 spectrophotometer, linked to a PC workstation running UV-Winlab software. Temperature was controlled ( $\pm 0.1$  °C) using either a Julabo U3 water circulator (Lambda 40) or a Perkin-Elmer PT01 Peltier system (Lambda 35). Protein concentrations (pH 7.0, 25 °C) were determined from the molar absorption coefficients ( $\epsilon = 8.8 \times 10^4 \text{ M}^{-1} \text{ cm}^{-1}$  for S160M<sub>R</sub>). The absorption coefficient for S160M<sub>G</sub> was obtained from comparison of the S160M<sub>R</sub> and S160M<sub>G</sub> spectra ( $\epsilon = 7.7 \times 10^4 \text{ M}^{-1} \text{ cm}^{-1}$  for S160M<sub>G</sub>). The molar absorption coefficient for rpAPX has been reported previously.<sup>19</sup>

**High Performance Liquid Chromatography.** All HPLC assays were conducted on a Varian Star HPLC system with an analytical Vydac C18 reverse phase HPLC column under PC control. Solvents were as follows: A = 0.1% w/v trifluoroacetic acid (TFA) in  $\text{H}_2\text{O}$ ; B = 0.1% v/v TFA in MeCN. Enzyme (10  $\mu\text{L}$ ) was mixed with an equal volume of 2% SDS. After 1 h, the sample was increased to 110  $\mu\text{L}$  total volume with  $\text{H}_2\text{O}$  and injected (100  $\mu\text{L}$ ) onto the column which had been preequilibrated with buffer A. Protein/heme separation was achieved using the following elution gradient: 30–42% B for 36 min, 42% A for 10 min, 42–100% B for 1 min followed by a washing sequence. UV detection was at 215 nm for protein and 404 nm for heme.

**Mass Spectrometry.** Samples for electrospray mass spectrometry were analyzed using a micromass Quattro BQ (Tandem Quadrupole) mass spectrometer. Horse heart myoglobin was used to calibrate the instrument in the range 600–1800 *m/z*. Samples of enzyme were exhaustively exchanged into deionized  $\text{H}_2\text{O}$  and diluted with MeOH containing 0.1% acetic acid and were introduced into the instrument at a flow rate of 5  $\mu\text{L min}^{-1}$ .

Samples for trypsin digestion were treated with 50:1 w/w (enzyme: trypsin) in ammonium bicarbonate buffer (0.4 M, pH 8.0, 37 °C) for 18 h. The digest mixture was injected onto a 1 mm diameter reversed phase C18 MS-HPLC column (Vydac); solvents were as follows: A = 0.01% w/v TFA in  $\text{H}_2\text{O}$ ; B = 0.01% w/v TFA in 80% MeCN, 20%  $\text{H}_2\text{O}$ . Peptide separation was achieved with a linear gradient of 2–100% B over 80 min, monitoring at 215 nm (protein) and 404 nm (heme). Peptide fractions showing both heme and protein absorbances were evaporated to dryness and then dissolved in  $\text{H}_2\text{O}$  (25  $\mu\text{L}$ ). These samples (1  $\mu\text{L}$ ) were then mixed with 1  $\mu\text{L}$  of matrix ( $\alpha$ -cyano-4-hydroxycinnamic acid, saturated solution, 1:1 MeCN/ $\text{H}_2\text{O}$ , 0.2% TFA) for MALDI-TOF mass spectrometry.

- (12) LeBrun, L. A.; Xu, F.; Kroetz, D. L.; Ortiz de Montellano, P. R. *Biochemistry* **2002**, *41*, 5931–5937.
- (13) Henne, K. R.; Kunze, K. L.; Zheng, Y.-M.; Christmas, P.; Soberman, R. J.; Rettie, A. E. *Biochemistry* **2001**, *40*, 12925–12931.
- (14) DePillis, G. D.; Ozki, S.; Kuo, J. M.; Maltby, D. A.; Ortiz de Montellano, P. R. *J. Biol. Chem.* **1997**, *272*, 8857–8860.
- (15) Colas, C.; Kuo, J. M.; Ortiz de Montellano, P. R. *J. Biol. Chem.* **2002**, *277*, 7191–7200.
- (16) Colas, C.; Ortiz de Montellano, P. R. *J. Biol. Chem.* **2004**, *279*, 24131–24140.
- (17) Lad, L.; Mewies, M.; Basran, J.; Scrutton, N. S.; Raven, E. L. *Eur. J. Biochem.* **2002**, *369*, 3182–3192.

- (18) Dalton, D. A.; Diaz del Castillo, L.; Kahn, M. L.; Joyner, S. L.; Chatfield, J. M. *Arch. Biochem. Biophys.* **1996**, *328*, 1–8.
- (19) Hill, A. P.; Modi, S.; Sutcliffe, M. J.; Turner, D. D.; Gilfoyle, D. J.; Smith, A. T.; Tam, B. M.; Lloyd, E. *Eur. J. Biochem.* **1997**, *248*, 347–354.

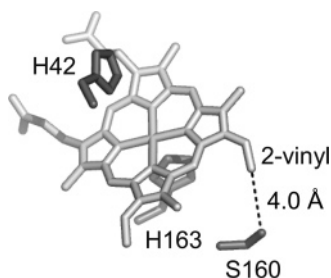


**Figure 2.** The structure of rpAPX.<sup>21</sup> The heme, the proximal (H163) and distal (H42) residues, serine 160, and the 2-vinyl group of the heme are indicated.

Analysis of the peptide–heme adducts by MALDI-TOF mass spectrometry was carried out as follows: 1  $\mu$ L of the 1:1 peptide/matrix mixture was spotted onto a MALDI target plate using the drying droplet method. The MALDI-TOF mass spectrometer was calibrated in the range 500–4500 Da with a peptide mass calibration kit (Sigma, used according to manufacturer's instructions) or using the known mass of the S160M variant. Spectra of the tryptic digests were collected in the same mass range using an average of at least 100 laser shots. The spectra were analyzed using Data Viewer software (Applied Biosystems).

**Steady State and Transient Kinetics.** Steady-state measurements (sodium phosphate buffer pH 7.0,  $\mu = 0.10$  M, [enzyme]  $\approx 25$  nM, 25.0  $^{\circ}$ C) were carried out according to published procedures.<sup>20</sup> Data were fitted to the Michaelis–Menton equation. Quoted  $k_{\text{cat}}$  and  $K_{\text{M}}$  values are averages of at least three kinetic runs.

Transient state kinetics were performed using a SX.18 MV micro-volume stopped-flow spectrophotometer (Applied Photophysics Ltd.) fitted with a Neslab RTE200 circulating water bath ( $\pm 0.1$   $^{\circ}$ C). All experiments were carried out using 100 mM potassium phosphate buffer, pH 7.0, 25.0  $^{\circ}$ C. Kinetic data were analyzed using nonlinear least-squares regression analysis on an Archimedes 410-1 micro-computer, using spectra-kinetics software. Formation of Compound I ( $k_1$ ) for S160M<sub>R</sub> was monitored under second-order conditions at 406 nm; the subsequent decay of Compound I ( $k_2$ ) was monitored at 408 nm. All rate constants reported were averages of at least five kinetic runs. Time-dependent spectra were obtained by multiple wavelength stopped-flow spectroscopy using a photodiode array detector and x-scan software (Applied Photophysics Ltd.). Spectral intermediates were obtained using singular value decomposition and PROKIN software (Applied Photophysics Ltd.).

## Results

**Molecular Modeling.** Analysis of the crystal structure of recombinant pea cytosolic APX (rpAPX)<sup>21</sup> identified Ser160 as a prime candidate for mutagenesis. The crystal structure reveals that the hydroxyl group of the serine 160 residue is positioned 4.0  $\text{\AA}$  away from the  $C_{\beta}$  of the 2-vinyl group of the heme, Figure 2. Molecular modeling and energy minimization showed that the sulfur atom of the Met160 residue in the S160M model structure could be placed within 1–1.5  $\text{\AA}$  of the  $C_{\beta}$  of the 2-vinyl group of the heme (data not shown).

**Characterization of S160M<sub>R</sub>.** The S160M variant was expressed as a colorless *apo*-enzyme, which after reconstitution with hemin gives a red enzyme (S160M<sub>R</sub>) with a UV–visible spectrum ( $\lambda_{\text{max}}/\text{nm}$  ( $\epsilon/\text{mM}^{-1} \text{cm}^{-1}$ ) = 407 (88),  $\sim 511$ ,  $\sim 532$ , 633) (pH 7.0,  $\mu = 0.10$  M, 25.0  $^{\circ}$ C), Figure 3, similar to that of rpAPX ( $\lambda_{\text{max}}/\text{nm}$  = 406.5, 504, and 634.5). The ESI mass spectrum of S160M<sub>R</sub> gives a mass of  $28\,507.6 \pm 1.93$  Da (calculated mass for *apo*-S160M = 28 504.18 Da), Figure 4A,

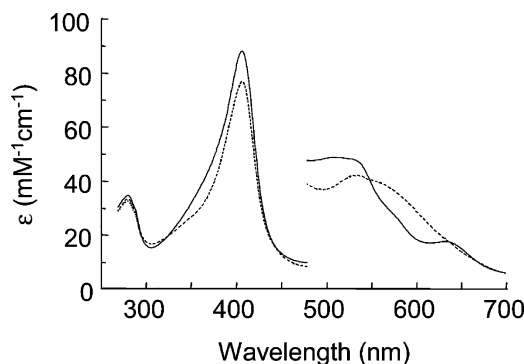


**Figure 3.** UV–visible spectra of S160M<sub>R</sub> (solid line) and S160M<sub>G</sub> (dashed line). The visible region of the spectrum has been multiplied by a factor of 5. Conditions: 100 mM phosphate, pH 7.0.

indicating that no posttranslational modification has occurred and that the heme is not covalently linked to the protein.

Steady-state oxidation (pH 7.0,  $\mu = 0.10$  M, 25.0  $^{\circ}$ C) of ascorbate by S160M<sub>R</sub> gives steady-state parameters ( $k_{\text{cat}} = 156 \pm 7$  s<sup>-1</sup>,  $K_{\text{M}} = 102 \pm 15$   $\mu$ M) that are comparable to those obtained for rpAPX ( $k_{\text{cat}} = 159 \pm 5$  s<sup>-1</sup>,  $K_{\text{M}} = 355 \pm 31$   $\mu$ M), indicating S160M<sub>R</sub> is catalytically competent in the presence of substrate. No formation of S160M<sub>G</sub> (as evidenced by electronic spectroscopy and HPLC, data not shown) is observed in the presence of ascorbate.

**Formation and Characterization of S160M<sub>G</sub>.** Reaction of S160M<sub>R</sub> with 1.5 equiv of H<sub>2</sub>O<sub>2</sub> in the absence of any reducing substrate results, over a period of minutes, in conversion to a green enzyme (S160M<sub>G</sub>) with a UV–visible spectrum ( $\lambda_{\text{max}}/\text{nm}$  ( $\epsilon/\text{mM}^{-1} \text{cm}^{-1}$ ) = 409 (77), 535, 565<sup>sh</sup>) (pH 7.0,  $\mu = 0.10$  M, 25.0  $^{\circ}$ C), Figure 3, that is distinct from that of either S160M<sub>R</sub> or rpAPX. Myeloperoxidase is also green.

Confirmation of covalent attachment in S160M<sub>G</sub> was three-fold. First, an acidified butanone extraction<sup>22</sup> did not remove the heme from the protein; in contrast, control experiments with both rpAPX and S160M<sub>R</sub> showed complete heme extraction into the organic layer (data not shown). Second, HPLC experiments showed that both the heme (measured at 404 nm) and the protein (measured at 215 nm) components coeluted at 39 min in S160M<sub>G</sub>, whereas in S160M<sub>R</sub> the heme is released from the protein and elutes earlier (27 min) than the protein peak (39 min), Figure 5. Coelution is indicative of covalent heme attachment and is seen in other covalently linked species such as lactoperoxidase.<sup>6</sup> In control experiments with rpAPX (data not shown), the heme was found to elute earlier (28.4 min) than the protein (41.6 min), analogous to the behavior seen for S160M<sub>R</sub> (above); a commercial sample of hemin eluted at 28.7 min (data not shown). In pH-dependent experiments, the formation of the covalent product was not affected by pH in the range 5.0–8.5 (as evidenced by HPLC analysis), but this was not examined in further detail. In further control experiments, a 1:1 mixture of S160M<sub>R</sub> and S160M<sub>G</sub> was observed to show two peaks by anion-exchange FPLC, Figure 4B: in this case, S160M<sub>G</sub> elutes before S160M<sub>R</sub>, which is consistent with the presence of a sulfonium ion linkage in S160M<sub>G</sub> (increased positive charge).

Mass spectrometry provided further evidence that the heme prosthetic group in S160M<sub>G</sub> was covalently linked to the protein

(20) Lad, L.; Mewies, M.; Raven, E. L. *Biochemistry* **2002**, *41*, 13774–13781.  
(21) Patterson, W. R.; Poulos, T. L. *Biochemistry* **1995**, *34*, 4331–4341.

(22) Teale, F. W. J. *Biochim. Biophys. Acta* **1959**, *35*, 543.



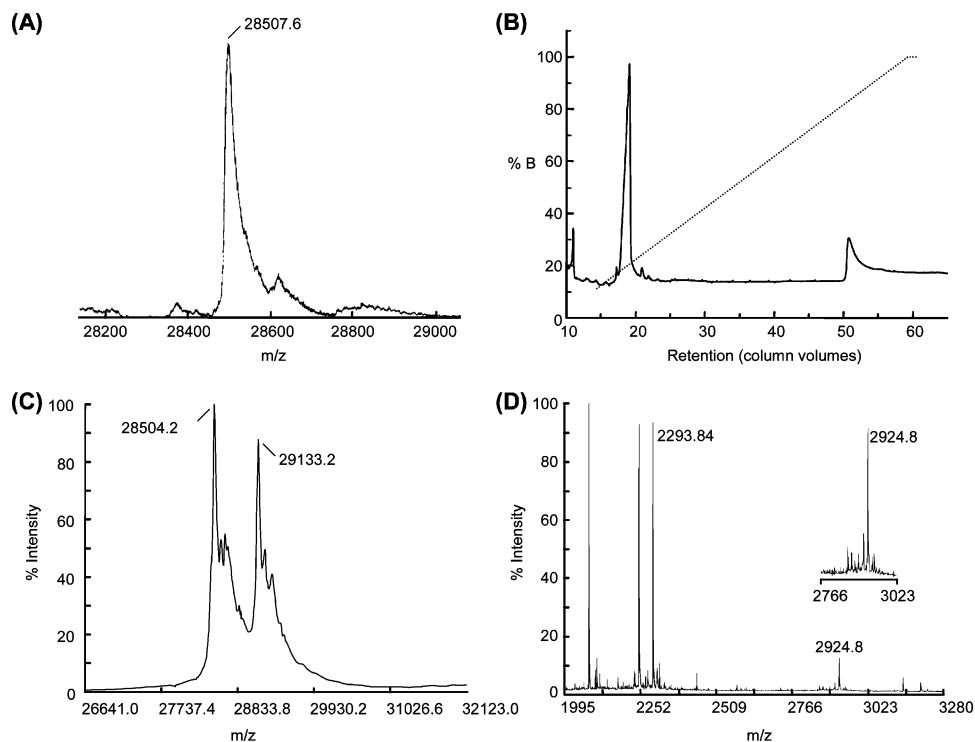


**Figure 4.** (A) Electrospray mass spectrum of S160M<sub>R</sub>. (B) FPLC separation of a 1:1 mixture of S160M<sub>R</sub> and S160M<sub>G</sub>. Protein was eluted using a linear gradient of 1 M KCl (shown as %B on y-axis). (C) MALDI-TOF mass spectrum of a 1:1 mixture of S160M<sub>R</sub> and S160M<sub>G</sub>. (D) MALDI-TOF mass spectrum of the heme-containing fragment of S160M<sub>G</sub> after digestion with trypsin and HPLC separation.

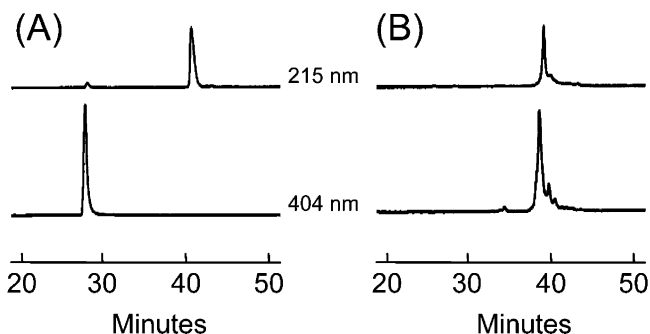
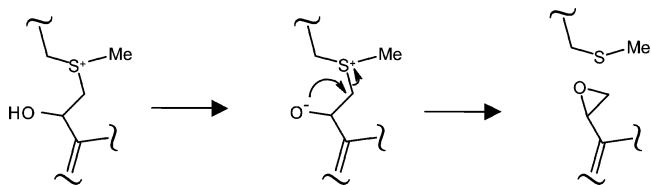


**Figure 5.** HPLC analysis of (A) S160M<sub>R</sub> and (B) S160M<sub>G</sub> at 215 and 404 nm.

backbone. MALDI-TOF mass spectrometry of the same 1:1 mixture of S160M<sub>R</sub> and S160M<sub>G</sub> that was used for the FPLC analysis (Figure 4B, above) gave a peak at 29 133.2 Da, Figure 4C, which is 629 Da higher than the mass of S160M<sub>R</sub> (28 504 Da, Figure 4C and above) and is consistent with the covalent attachment of heme to the protein (expected mass increase 633.52). Tryptic digestion of S160M<sub>G</sub> was also carried out and followed by isolation of the component of the resulting reaction mixture that showed both peptide (measured at 215 nm) and heme (measured at 404 nm) absorbance upon separation by HPLC. MALDI-TOF mass spectrometry of this separated component, which was visibly colored, gave a spectrum with a peak at 2924.8 Da, which is 15.3 Da higher than the calculated mass of 2909.5 Da expected for the AMGLSDQDI-VALM<sup>160</sup>GGHTIGAHK fragment covalently bound to the heme through a methionine–vinyl sulfonium link. This is consistent with the presence of an additional hydroxyl group. Significantly, no peak at 616 Da, corresponding to free heme, is observed for this fragment, indicating the absence of noncovalently bound

#### Scheme 1. Proposed Mechanism of Formation of Heme Epoxide



heme in the sample. The presence of a ferric-hydroxide heme<sup>23</sup> is not consistent with the +15.3 mass increase because MALDI-TOF analysis of rpAPX shows a peak for free heme without any ligand bound (data not shown). An additional peak is observed at 2293.8 Da in the MALDI-TOF spectrum, which corresponds to the mass of the free peptide (calculated 2293.1). In subsequent experiments, we observed that the intensity of the 2924.8 peak decreased with increasing laser power, which we believe is due to laser-induced breakdown of this heme fragment into the free peptide and a heme epoxide product that was also detected at 632.23 Da (calculated 632.52 Da, data not shown). Scheme 1 shows the proposed mechanism of this breakdown, which occurs more readily at higher laser power settings. This is not observed during MALDI-TOF analyses of the intact S160M<sub>G</sub> enzyme (Figure 4C, above).

To provide further information on the location of covalent attachment on the heme, *apo*-S160M was reconstituted with iron(III) mesoporphyrin (mesoheme), in which alkyl groups replace the 2- and 4-vinyl groups, and reacted with H<sub>2</sub>O<sub>2</sub> as above. In this case, no covalent heme product was obtained (as evidenced by acidified butanone extraction and HPLC, data not shown). Because rpAPX also gives no covalent product, these data indicate that both Met160 and one of the vinyl groups must be present for covalent attachment to occur.

(23) Colas, C.; Ortiz de Montellano, P. R. *Chem. Rev.* **2003**, *103*, 2305–2332.

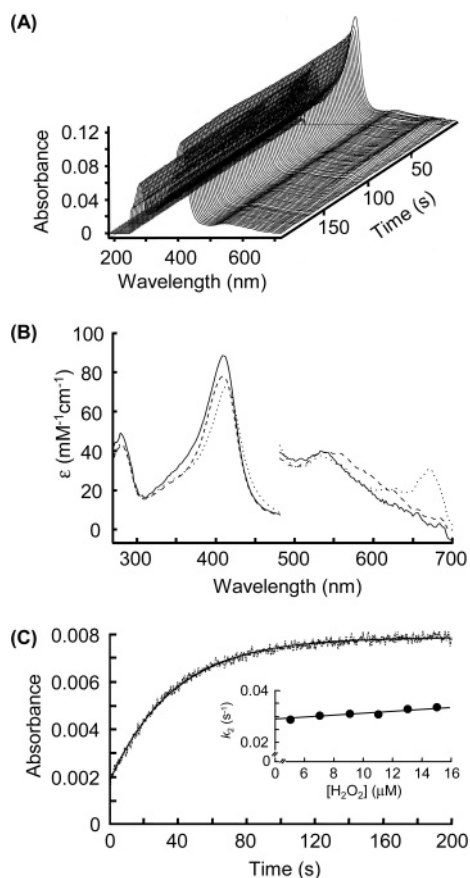


**Figure 6.** Reaction of S160M<sub>R</sub> with H<sub>2</sub>O<sub>2</sub> monitored using stopped flow and photodiode array spectroscopy (pH 7.0, 25.0 ± 0.1 °C). (A) Photodiode array spectra collected over 200 s following rapid mixing of S160M<sub>R</sub> with H<sub>2</sub>O<sub>2</sub>. For clarity, only every fifth spectrum is shown. (B) Deconvoluted spectra of the intermediates resolved from singular value decomposition analysis of the spectra shown in (A). The solid line corresponds to the spectrum of S160M<sub>R</sub>, the dotted line corresponds to the Compound I intermediate, and the dashed line corresponds to S160M<sub>G</sub>. The visible region of the spectrum has been multiplied by a factor of 5. Conditions: [S160M<sub>R</sub>] = 1 μM, [H<sub>2</sub>O<sub>2</sub>] = 1 μM. (C) Monophasic absorbance change at 408 nm determined in single wavelength mode. The solid line is a fit of the data to a first-order, single-exponential process. Inset: dependence of the first-order rate constant,  $k_2$ , on concentration of H<sub>2</sub>O<sub>2</sub>. The solid line is a fit of the data to  $y = mx + c$ . Error bars are contained within the black circles representing the rate constants. Conditions: [S160M<sub>R</sub>] = 1 μM, [H<sub>2</sub>O<sub>2</sub>] = 5 μM.

**Kinetic Studies.** Stopped-flow and photodiode array experiments (pH 7.0,  $\mu = 0.10$  M, 4.0 °C) show that the conversion of S160M<sub>R</sub> to S160M<sub>G</sub> is biphasic, Figure 6A. After rapid mixing of S160M<sub>R</sub> (1 μM) with H<sub>2</sub>O<sub>2</sub> (1 μM), a rapid decrease in absorbance in the Soret peak is observed, and a new peak at ~670 nm appears. This is followed by the (slow) appearance of a new species with a maximum at ~540 nm, which corresponds to the spectrum of S160M<sub>G</sub> obtained above (Figure 3). Time-dependent spectra obtained in Figure 6A can be processed by singular value decomposition analysis to identify spectral intermediates. The globally analyzed spectra were best fit to a model  $A \rightarrow B \rightarrow C$  with three distinct spectral intermediates, Figure 6B, where A corresponds to S160M<sub>R</sub> ( $\lambda_{\text{max}} = 409, 534$  nm), B corresponds to the spectrum of the intermediate ( $\lambda_{\text{max}}/\text{nm} = 414, 534, 670$ ) and C corresponds to S160M<sub>G</sub> ( $\lambda_{\text{max}}/\text{nm} = 410, 534, 557$ ). The wavelength maxima for the deconvoluted spectra of A and C are in reasonable agreement with those obtained above using conventional

electronic spectroscopy. The decrease in intensity in the Soret region and the increase in absorbance at ~670 nm of the intermediate is characteristic of the Compound I derivative of rpAPX ( $\lambda_{\text{max}}/\text{nm} = 404, 529, 583, 650^{17}$ ) and recombinant soybean cytosolic APX ( $\lambda_{\text{max}}/\text{nm} = 409, 530, 569, 655^{17}$ ), both of which are known to contain a porphyrin  $\pi$ -cation radical. The Compound I intermediate has a longer lifetime than Compound I in either rpAPX or rsAPX, however. This means that it is also observable using conventional UV–visible spectroscopy (data not shown): wavelength maxima ( $\lambda_{\text{max}}/\text{nm} = 411, 529, 562^{\text{sh}}, 668$ ) obtained in this way were similar to those observed from the SVD analysis.

Single-wavelength stopped-flow experiments showed that the first (fast) step is second order overall with a first-order (linear) dependence on the concentration of H<sub>2</sub>O<sub>2</sub> (data not shown). For this first stage involving Compound I formation, 88–94% of the theoretical maximum absorbance change is observed. Significant heme degradation occurred with high ([H<sub>2</sub>O<sub>2</sub>] > 20 × [S160M<sub>R</sub>]) concentrations of H<sub>2</sub>O<sub>2</sub> (in the absence of substrate): this is almost certainly due to the reaction of Compound I with excess H<sub>2</sub>O<sub>2</sub> and is known to lead to enzyme inactivation. (This is not incompatible with the activity of the enzyme in the steady state (see above), because the presence of substrate protects against inactivation<sup>24</sup> at concentrations that are lower than those used to determine  $k_{\text{cat}}$  in this paper. We assume that, under steady-state conditions, reaction of the enzyme with excess H<sub>2</sub>O<sub>2</sub> is not competitive with reduction by substrate.) Hence, the rate constant,  $k_1$ , for Compound I formation was measured under second-order ([S160M<sub>R</sub>] = [H<sub>2</sub>O<sub>2</sub>] = 1–5 μM), rather than pseudo-first-order ([H<sub>2</sub>O<sub>2</sub>] ≫ [S160M<sub>R</sub>]), conditions ( $k_1 = (4.3 \pm 0.69) \times 10^8 \text{ M}^{-1} \text{ s}^{-1}$  for S160M<sub>R</sub> as compared to  $k_1 = (2.7 \pm 5.4) \times 10^8 \text{ M}^{-1} \text{ s}^{-1}$  for rpAPX under identical conditions).

The second (slow) step of the reaction shows absorbance changes that fit to a first-order process, Figure 6C. In this case, the observed absorbance change of  $\sim 6.3 \times 10^{-3}$  is consistent with the expected change in absorbance ( $\Delta\text{Abs} \approx 7 \times 10^{-3}$ , calculated from the difference in calculated absorption coefficients between the Compound I intermediate and S160M<sub>G</sub> at this wavelength ( $\Delta\epsilon \approx 7.6 \text{ mM}^{-1} \text{ cm}^{-1}$ ), Figure 6B). The first-order rate constant,  $k_2$ , obtained from an average of the rate constants obtained at different concentrations of H<sub>2</sub>O<sub>2</sub> is  $0.034 \pm 0.2 \text{ s}^{-1}$  and is essentially independent of the concentration of H<sub>2</sub>O<sub>2</sub> (zero order in [H<sub>2</sub>O<sub>2</sub>]) in the range 0–15 μM, Figure 6C, inset. This second stage is slow in comparison with reduction of Compound I by ascorbate ( $k = 2.7 \times 10^7 \text{ M}^{-1} \text{ s}^{-1}$  for rpAPX<sup>20</sup>) or with the steady-state oxidation of ascorbate (above),<sup>25</sup> which accounts for the normal catalytic behavior of S160M<sub>R</sub> in the presence of ascorbate.

## Discussion

The development of our understanding of heme structure in the mammalian peroxidases has been much slower than in the plant peroxidase enzymes and has been hampered by the difficulties associated with extraction of the heme group from the polypeptide. Lactoperoxidase has served as a benchmark in this area. It was known from early work on LPO<sup>1,4</sup> that the

(24) Hiner, A. N. P.; Rodriguez-Lopez, J. N.; Arnao, M. B.; Raven, E. L.; Garcia-Canovas, F.; Acosta, M. *Biochem. J.* **2000**, *348*, 321–328.

(25) Reduction of Compound II,  $k_3$ , is rate-limiting in the APX mechanism, so that  $k_3$  approximates to  $k_{\text{cat}}$ .

heme was bound to the protein through a covalent link because treatment with acidified butanone failed to extract the heme under conditions that were known to lead to heme extraction in other, noncovalently bound enzymes. Numerous proposals were put forward for the heme structure, including ester- and amide-linked hemes and disulfide-bound heme,<sup>2–4</sup> but the precise heme structure has only recently been established,<sup>5,6</sup> Figure 1. In the case of myeloperoxidase, there is an additional sulfonium link from the C $\beta$  of the 2-vinyl group to a methionine residue, Figure 1. There is no indication at present as to what specific properties these covalent linkages confer upon the heme group, how the reactivity of the heme group is affected, or how this is connected to functional activity. In addition, obtaining detailed information on the mechanism of formation of these linkages has been prohibitively difficult for either LPO or MPO (as well as for other mammalian peroxidases) because (a) the isolation procedures for native enzymes produce enzyme in which the covalent links are already formed, and (b) because the recombinant expression systems that are available produce enzyme in which the covalent links are either already formed (for MPO<sup>26,27</sup>) or which are incompletely formed and require further processing (for LPO<sup>14,28</sup>). The results presented here provide the first evidence for a covalent heme–methionine link in a non-mammalian peroxidase enzyme. The covalent link is analogous to the link found in MPO and provides, to our knowledge, the first direct information on the likely reaction mechanism.

Scheme 2 depicts one possible mechanism for formation of S160M<sub>G</sub> that is consistent with all of the data obtained in this work. In this proposed mechanism, we have detected the Compound I intermediate directly; after step (i), the intermediates are speculative. The essentials are as follows:

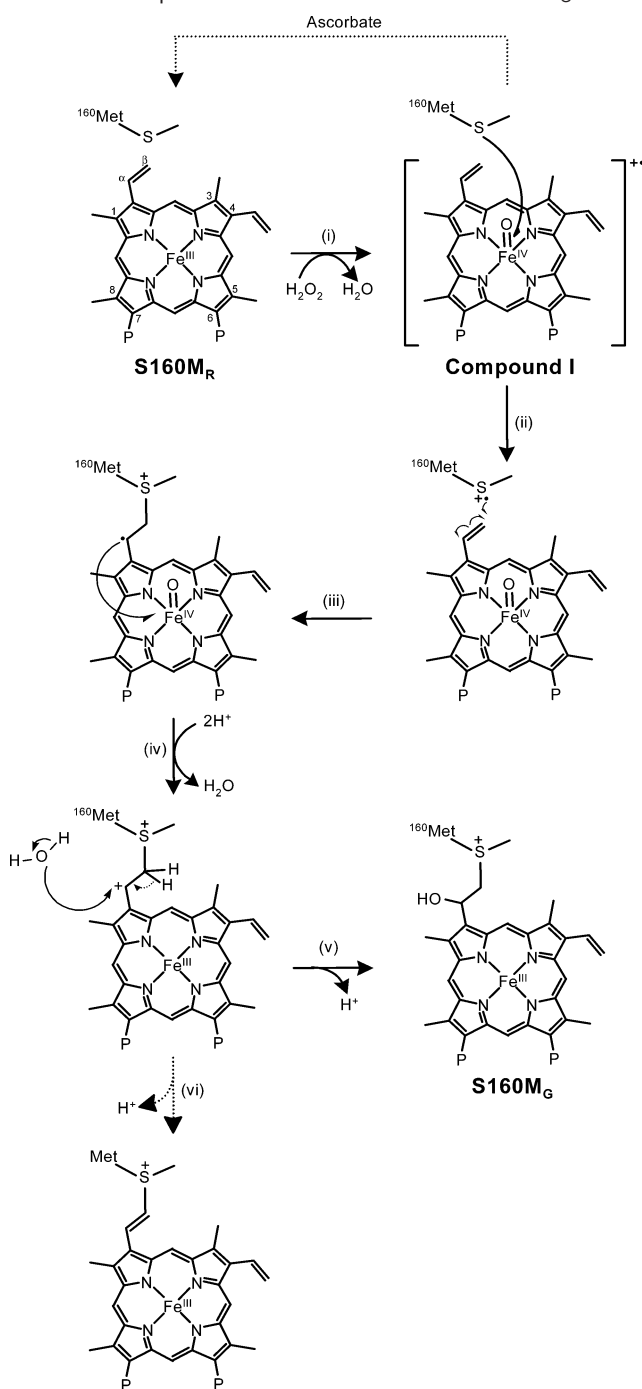
(i) Reaction of S160M<sub>R</sub> with H<sub>2</sub>O<sub>2</sub> gives Compound I, containing a porphyrin  $\pi$ -cation intermediate. Under steady-state conditions (in the presence of excess ascorbate), normal catalytic activity is observed for S160M<sub>R</sub>: this Compound I intermediate must therefore be reduced by ascorbate so that formation of S160M<sub>G</sub> is not observed in the presence of substrate.

(ii) One-electron reduction by Met160 gives a protein-based radical cation (Met<sup>•+</sup>). There is precedent for this step because extensive evidence exists for peroxidase-catalyzed (including MPO-catalyzed<sup>29</sup>) oxidation of various sulfides,<sup>30</sup> and there is mechanistic evidence for radical cation (S<sup>•+</sup>) formation.<sup>31,32</sup>

(iii) Addition of the radical across the C $\beta$  of the double bond of the 2-vinyl group results in a stable, conjugated (secondary) radical on C $\alpha$ . (Radical attack at C $\alpha$  would give a primary, nonconjugated radical at this stage, which is predicted to be less stable.)

(iv) Reduction of the ferryl heme by this radical gives a (secondary) carbocation at C $\alpha$  and release of H<sub>2</sub>O according to the normal peroxidase cycle.

**Scheme 2.** Proposed Mechanism of Formation of S160M<sub>G</sub><sup>a</sup>



<sup>a</sup> Species detected in this work are indicated in bold text; other species are speculative. Reactions i–vi are described in the text.

(v) Nucleophilic attack of H<sub>2</sub>O gives a heme structure that is consistent with the mass spectrometric data, indicating addition of a hydroxyl group.

(vi) For MPO, addition of a hydroxyl group clearly does not occur, and an alternative pathway, involving loss of H<sup>+</sup> from the same cation intermediate and retention of the double bond, has been suggested.<sup>23</sup> The loss of this double bond in S160M<sub>G</sub> may account for the fact that S160M<sub>G</sub> shows no significant red shift in the Soret band; in MPO, this shift has been attributed to the conjugation of the sulfonium ion with the heme group.<sup>9</sup>

There are clearly aspects of this reaction mechanism that require more detailed investigation, but these results demonstrate

- (26) Jacquet, A.; Garcia-Quintana, L.; Dellersnyder, V.; Fenna, R. E.; Bollen, A.; Moguilevsky, N. *Biochem. Biophys. Res. Commun.* **1994**, *202*, 73–81.  
 (27) Kooter, I. M.; Moguilevsky, N.; Bollen, A.; Sijtsema, N. M.; Otto, C.; Wever, R. J. *Biol. Inorg. Chem.* **1997**, *2*, 191–197.  
 (28) Watanabe, Y.; Varsolona, F.; Yoo, Y.-C.; Guillaume, J.-P.; Bollen, A.; Shimazaki, K.; Moguilevsky, N. *FEBS Lett.* **1998**, *441*, 476–479.  
 (29) Burner, U.; Jantschko, W.; Obinger, C. *FEBS Lett.* **1999**, *443*, 290–296.  
 (30) See, for example: Holland, H. L. *Nat. Prod. Rep.* **2001**, *18*, 171–181.  
 (31) Baciocchi, E.; Lanzalunga, O.; Malandrucchi, S. *J. Am. Chem. Soc.* **1996**, *118*, 8973–8974.  
 (32) Kobayashi, S.; Nakano, M.; Kimura, T.; Schaap, A. P. *Biochemistry* **1987**, *26*, 5019–5022.

that the strategic positioning of a suitable methionine residue close to the heme and contained within a catalytically competent structural architecture is sufficient for methionine–heme cross-linking to occur. This raises the intriguing possibility that, in principle, any heme peroxidase with appropriately positioned residues can duplicate the active site architecture observed in the mammalian peroxidases. If this is the case, it would provide an alternative route for exploring the effects of these covalent linkages on heme function that avoids the inherent

experimental complications associated with the mammalian peroxidase enzyme.

**Acknowledgment.** We thank Dr. Martin Mewies for construction of the His-tag vector and Dr. Sandeep Handa for helpful discussions. This work was supported by The Wellcome Trust (grants 062641/Z/00/Z and 063688/Z/01/Z).

JA048242C